



Radiographic and histopathological study of gastrointestinal dysmotility in lipopolysaccharide-induced sepsis in the rat

Marta Castro^{1,2,3} | Marta Sofía Valero^{1,2,3} | Yolanda López-Tofiño^{4,5} |
 Laura López-Gómez^{5,6} | Rocío Girón^{4,7,8} | María Isabel Martín-Fontelles^{4,8,9} |
 José A. Uranga^{5,6}  | Raquel Abalo^{4,5,8,9,10} 

¹Departamento de Farmacología, Fisiología y Medicina Legal y Forense, Universidad de Zaragoza, Zaragoza, Spain

²Instituto de Investigación Sanitaria de Aragón (IIS Aragón), Zaragoza, Spain

³Instituto Agroalimentario de Aragón (IA2), Universidad de Zaragoza-CITA, Zaragoza, Spain

⁴Área de Farmacología y Nutrición, Departamento de Ciencias Básicas de la Salud, Universidad Rey Juan Carlos (URJC), Alcorcón, Spain

⁵High-Performance Research Group in Physiopathology and Pharmacology of the Digestive System (NeuGut-URJC), Alcorcón, Spain

⁶Área de Histología Humana y Anatomía Patológica, Departamento de Ciencias Básicas de la Salud, Universidad Rey Juan Carlos (URJC), Alcorcón, Spain

⁷High-Performance Research Group in Experimental Pharmacology (PHARMAKOM-URJC), Alcorcón, Spain

⁸Unidad Asociada I+D+i del Instituto de Química Médica (IQM), Consejo Superior de Investigaciones Científicas (CSIC), Madrid, Spain

⁹Grupo de Trabajo de Ciencias Básicas en Dolor y Analgesia de la Sociedad Española del Dolor, Madrid, Spain

¹⁰Grupo de Trabajo de Cannabinoides de la Sociedad Española del Dolor, Madrid, Spain

Correspondence

Raquel Abalo and José A. Uranga, Dpto. CC. Básicas de la Salud. Facultad de Ciencias de la Salud, Universidad Rey Juan Carlos, Avda Atenas s/n. 28922 Alcorcón-Madrid, Spain.
 Email: raquel.abalo@urjc.es and jose.uranga@urjc.es

Funding information

Comunidad de Madrid, Grant/Award Number: S-SAL/0261/2006 and S2010/BMD-2308; Fundación Ibercaja-Universidad de Zaragoza, Grant/Award Number: JIUZ-2015-BIO-02; Gobierno de Aragón, Grant/Award Number: B04_17R and B29_17R; Ministerio de Ciencia e Innovación, Grant/Award Number: SAF2012-40075-CO2-01; Ministerio de Ciencia, Innovación y Universidades, Grant/Award Number: AGL2017-82987-R and SAF2017-83120-C2-1-R; Universidad Rey Juan Carlos-Banco de Santander, Grant/Award Number: Call 2020 (NACfightsCOVID-19)

Abstract

Background: Sepsis is a highly incident condition in which a cascade of proinflammatory cytokines is involved. One of its most frequent consequences is ileus, which can increase mortality. Animal models such as that induced by systemic administration of lipopolysaccharide (LPS) are useful to deeply evaluate this condition. The effects of sepsis on the gastrointestinal (GI) tract have been explored but, to our knowledge, in vivo studies showing the motor and histopathological consequences of endotoxemia in an integrated way are lacking. Our aim was to study in rats the effects of sepsis on GI motility, using radiographic methods, and to assess histological damage in several organs.

Methods: Male rats were intraperitoneally injected with saline or *E. coli* LPS at 0.1, 1, or 5 mg kg⁻¹. Barium sulfate was intragastrically administered, and X-rays were performed 0–24 h afterwards. Several organs were collected for organography, histopathology, and immunohistochemistry studies.

Key Results: All LPS doses caused gastroparesia, whereas changes in intestinal motility were dose- and time-dependent, with an initial phase of hypermotility followed by paralytic ileus. Lung, liver, stomach, ileum, and colon (but not spleen or kidneys) were damaged, and density of neutrophils and activated M2 macrophages and expression of cyclooxygenase 2 were increased in the colon 24 h after LPS 5 mg kg⁻¹.

This is an open access article under the terms of the [Creative Commons Attribution-NonCommercial](https://creativecommons.org/licenses/by-nc/4.0/) License, which permits use, distribution and reproduction in any medium, provided the original work is properly cited and is not used for commercial purposes.

© 2023 The Authors. *Neurogastroenterology & Motility* published by John Wiley & Sons Ltd.

Conclusions and Inferences: Using radiographic, noninvasive methods for the first time, we show that systemic LPS causes dose-, time-, and organ-dependent GI motor effects. Sepsis-induced GI dysmotility is a complex condition whose management needs to take its time-dependent changes into account.

KEYWORDS

cytokine storm, gastrointestinal motility, immunohistochemistry, lipopolysaccharides, sepsis

1 | INTRODUCTION

Sepsis is a severe systemic reaction, with generalized inflammation, that occurs, among others, in response to infection of either bacterial or viral etiology. It affects 3–10 per 1000 inhabitants in the developed countries.¹ Although over the last years its mortality has decreased around 20%–30%, due to the knowledge of its pathophysiology and management improvements,^{2–4} sepsis is a risk factor for the development of gastrointestinal (GI) conditions, including gastroparesis, diarrhea, or ileus.^{5,6} Impaired GI motor function needs to be rapidly solved, as the degree of dysmotility is in relation with the severity of illness and mortality.⁷ Besides, rapid resolution permits enteral feeding, which is the recommended nutritional method if tolerated.^{8,9} International Guidelines for Management of Sepsis and Septic Shock 2016 establish several recommendations regarding gut dysmotility of these patients. They recommend the measurement of gastric residual or the use of prokinetics in patients with feeding intolerance (who are at risk of aspiration).⁸

Among others, sepsis can be developed by the presence in blood of constituents of bacteria, like lipopolysaccharide (LPS), a highly antigenic component of gram-negative bacteria outer membrane. Accordingly, sepsis and its effects on GI motility have been previously studied in preclinical models through the experimental administration of LPS. These effects are variable. In rodents, LPS delays gastric emptying and increases small intestinal transit^{10–12} or induces ileus¹³ by activating macrophages.¹⁴ In the dog, LPS at a single sublethal dose delays gastric emptying and colonic transit of solids¹⁵ or induces diarrhea and an increase in colonic transit of liquids.¹⁶ In sheep, LPS abolishes gastric antrum motility and impairs migrating motor complex.¹⁷ These apparently contradictory results may be due to the use of different doses and/or to the studies having been performed at different moments after LPS injection, but, to our knowledge, a comprehensive—from stomach to distal colon—in vivo minimally invasive investigation on the dynamic, dose-dependent changes occurring after LPS insult on GI motility in experimental animals is lacking. This is important to distinctly identify the different phases of the septic response to LPS, in which the cellular and molecular mechanisms involved, and, therefore, the treatments needed to prevent complications or mortality, may be different.

Radiographic methods applied after contrast administration in the conscious experimental animal may be very useful in order to study, in the same animal, these dynamic changes in transit.¹⁸ Moreover, these noninvasive methods allow for dynamic changes

Key Points

- Noninvasive radiographic methods were used to monitor the effects of sepsis induced by lipopolysaccharide (LPS) on gastrointestinal motility, and the damage caused in different organs was evaluated.
- Gastric emptying was delayed at all LPS doses, but the intestine was affected with increasing doses causing early hypermotility followed by paralytic ileus.
- Lung, liver, stomach, ileum, and colon were damaged, and density of neutrophils and M2 macrophages and expression of cyclooxygenase 2 were increased in the colon only at the highest dose tested.
- Systemic LPS causes dose-, time-, and organ-dependent gastrointestinal motor effects, not necessarily dependent on the degree of inflammation.

in other aspects of the GI viscera (size, contents appearance) to be easily evaluated.^{19–21} Thus, our aim was to radiographically study in the rat the dynamic changes induced by LPS on GI motility and general health parameters throughout the first 24 h after its systemic administration at different doses and to determine the associated histopathological alterations in several tissues.

2 | MATERIALS AND METHODS

2.1 | Animals and experimental protocol

Young adult male Wistar rats weighing 315–425 g were obtained from the Animal Facilities of Universidad Rey Juan Carlos (URJC), housed four animals/cage, and kept under controlled temperature, humidity, and dark/light conditions (22 ± 2°C, 55 ± 10% and 12/12 h, respectively, lights on at 8 am). They were fed ad libitum and had free access to water. Cages had standard bedding. All animal procedures were approved by the Ethics Committee from URJC and Comunidad Autónoma de Madrid (PROEX 061/18 and 173.6/21). Animal care and use were performed accordingly with the Spanish Policy for Animal Protection RD53/2013, which meets the European Union Directive 2010/63 on the protection of animals used for experimental and other scientific purposes.

All experiments started between 8:30 and 9:30am. Before procedures, animals were weighed. Lipopolysaccharide (LPS) from *Escherichia coli* O111:B4 was suspended in sterile 0.9% NaCl (vehicle) and intraperitoneally (i.p.) administered at 0 (control/saline, 0.5 mL/300g BW), 0.1, 1, or 5 mg kg⁻¹. Changes in GI motor function were monitored for 24h by radiographic means (see below). Rats were placed in clean cages (with standard bedding) after LPS administration (the same grouping was maintained in the clean cages, to avoid stress associated to isolation or mixing with other rats).

In addition, body weight and clinical status were surveyed at 8 and 24h after LPS. Thus, signs of dehydration were established by skin turgor evaluation²² (0: negative; 1: positive). General discomfort was inferred from the occurrence of vocalizations when holding the animals (0: no vocalization; 1: vocalization). The sum of these parameters was considered as a clinical score.

2.2 | Gastrointestinal Motility Evaluation

2.2.1 | Radiographic study

Radiographic methods (serial X-rays) were used for assessment of GI motor function as published before.^{18,20} Briefly, straight after saline or LPS administration, rats were gavaged 2.5 mL of a barium sulfate suspension (0.9 g/mL, room temperature) before taking the X-rays. A CS2100 (Carestream Dental, Spain) digital X-ray apparatus (60kV, 7 mA) was used. X-rays were recorded on Carestream Dental T-MATG/RA film (15×30cm) housed in a cassette provided with a regular intensifying screen film and were developed using a Kodak X-omat 2000 automatic processor. Exposure time was adjusted to 20–60ms. Animals were introduced in adjustable handmade transparent plastic tubes in order to restrict movement. Previous studies have shown that this restriction does not significantly alter GI motility parameters.¹⁸ To further reduce stress, rats were released immediately after each shot, so that immobilization lasted for 1–2 min.

Radiographs were taken at different time points (0, 1, 2, 4, 6, 8, and 24h) after LPS and contrast medium administration.

Analysis of X-rays was performed by two different trained investigators, blinded to drug administration, as previously reported.¹⁸ Briefly, a semiquantitative score (0–12 points) was calculated as the sum of the percentage of each GI region filled with contrast (0–4), intensity (0–4) and homogeneity of contrast (0–2) and sharpness (0–2) of the GI region profile. Thus, total score (for each rat, organ, and time point) was 0–12.

X-ray images also served to analyze alterations of stomach, cecum, and fecal pellets size or density, as well as to assess the number of fecal pellets visible within the colon. Changes in size could be due to mechanical alterations of GI wall or volume of contents and density may vary in relation to the degree of hydration of contents. For morphometric and densitometric analysis, an image analysis system (Image J 1.38 for Windows, U.S. National Institutes of Health, Bethesda, Maryland, USA, free software: <http://rsb.info.nih.gov/ij/>)

was employed as referred elsewhere.²³ For the morphometric analysis, area (the 2D projection of the organ in the X-ray images) was the parameter measured, as a surrogate of size (or volume).

The presence of abnormal content within the colorectal region, suggestive of diarrhea, was assessed from each X-ray at each time point. A classification of this barium-stained content was established as previously published (normal: presence of fecal pellets only; mildly abnormal: presence of both fecal pellets and liquid content; severely abnormal: presence of liquid content only).²¹ Data were expressed as % of animals having each type of content.

2.3 | Analysis of tissues

2.3.1 | Sample collection and macroscopic study

Twenty-four hours after LPS, animals received an i.p. overdose of sodium pentobarbital (60 mg kg⁻¹) and different organs were obtained at necropsy for macroscopic evaluation and histopathological analysis (see below).

The lungs of animals treated with saline or LPS 5 mg kg⁻¹ were obtained for histopathological examination, as a positive control of lung damage associated with sepsis²⁴ (due to technical issues, a different set of animals had to be used for this basic histologic study; in these animals, the clinical and GI effects were confirmed to be similar to those described here, but the results were not used in the present report).

The digestive organs (stomach, small, and large intestine) were removed *en bloc* and stretched out on top of a sheet of graph paper and photographed. Image J (the same software used for the X-ray quantitative analysis) was used to measure the areas (the 2D projection of the organ) of stomach (whole stomach, and body and forestomach, separately²⁵) and cecum, as well as the length of small intestine and colon, and values were normalized to body weight. The stomach was scored in a buoyancy test in saline (0: no buoyancy; 1: buoyancy).²⁶

Before storage for histopathological study, stomach, cecum, colon (all with contents), liver, spleen, and kidneys were weighed. These data are expressed normalized to body weight.

2.3.2 | Histopathological analysis

Samples from lungs, spleen, liver, kidney, esophagus, forestomach and stomach body, duodenum, terminal ileum, and proximal and distal colon were obtained, fixed in buffered 10% formalin and embedded in paraffin. Sections of 5 μm were stained with hematoxylin-eosin (HE). They were studied under a Zeiss Axioskop 2 microscope (Zeiss International, USA) equipped with the image analysis software package AxioVision 4.6 (Zeiss International) or LASX 3.7 (Leica Microsystems AG, Germany) to calculate the morphometric parameters (kidney glomerular area, and thickness of the lung alveolar wall, distal colon whole wall, and ileal and distal colon muscle layers). The

experimenter was blind to the treatment received by the rat from which the analyzed sample was obtained. Between 5 and 10 sections per animal were analyzed.

Histological damage was evaluated in sections of the ileum using criteria adapted from Sacconi et al. (2012).²⁷ A numerical score of 0–9 was assigned to each section considering general loss of mucosal architecture (graded 0–3, absent to severe), extent of inflammatory cell infiltrate (graded 0–3, absent to transmural), crypt abscess formation (0–1, absent or present), goblet cell depletion (0–1, absent or present), and muscular layer thickness (0–1, normal to reduced).

Histological damage was also evaluated in colonic sections using a semiquantitative score system according to Galeazzi et al. (1999), in which the following features were graded: damage of epithelium (0–3, normal to severe destruction), inflammatory cell infiltration (0–4, absent to severe), separation of muscular layer (0–2, normal to severe), and goblet cell depletion (0–4, no depletion to complete depletion).²⁸ Thus, a total numerical score of 0–13 points was assigned to each organ for each treatment.

Liver damage was evaluated according to the histological scoring system by Kleiner et al (2005).²⁹ Lung damage was evaluated according to Fahmi et al (2016),²⁴ and the thickness of the alveolar wall was measured under a 40× objective.

Immunohistochemistry was performed on colonic paraffin-embedded sections of 5 µm thickness. Deparaffined slides were washed with phosphate buffered saline (PBS) with 0.05% Tween 20 (Calbiochem, Darmstadt, Germany). Thereafter, sections were incubated for 10 min in 3% (v/v) hydrogen peroxide to inhibit endogenous peroxidase activity and blocked with serum for 30 min to minimize nonspecific binding of the primary antibody. Sections were then incubated overnight at 4°C with the following antibodies: antimacrophage-associated antigen CD163 (1:100, Santa Cruz Biotechnology, Inc., Santa Cruz, CA, USA) to quantify the number of activated M2 macrophages, antimyeloperoxidase (MPO) (Abcam, 1:1000, Cambridge, UK) to quantify neutrophils and anticyclooxygenase-2 antibody (COX-2) (Abcam, 1:1500, Cambridge, UK) to assess the presence of inflammation; similarly, anti-claudin-1 antibody (Abcam, 1:75, Cambridge, UK) was used to investigate epithelial barrier integrity. As a negative control, preparations were incubated without the primary antibody. After incubation, samples were washed with PBS-Tween. The peroxidase-based detection kit ImmPress (Vector labs, Burlingame, CA, USA) was used as chromogen. Samples were counterstained with hematoxylin and coverslips mounted with Eukitt mounting media (O. Kindler GmbH & Co, Freiburg, Germany). Quantification of the labeling was performed with Fiji-Image J software from a minimum of seven micrographs per sample.

2.4 | Compounds and drugs

Barium sulfate suspension (3.4 M barium sulfate, 88 mM sorbitol, 31 mM citric acid, 39 mM sodium citrate, and 180 mM arabic gum) was prepared in distilled water. Barium sulfate, sorbitol, arabic gum, and LPS were purchased from Sigma-Aldrich (Madrid, Spain).

Citric acid and sodium citrate were provided by Merck (Darmstadt, Germany) and Panreac (Barcelona, Spain), respectively.

2.5 | Statistical analysis

For the in vivo studies (evaluation of general health, gastrointestinal motility, and macroscopic features), *n* was initially set at 8–12 animals per experimental group. However, due to several technical issues (some unintentionally missing clinical and macroscopic data; some X-rays of not sufficient quality to allow for morphometric/densitometric analysis, despite usable for the semiquantitative evaluation; the lack of T24 X-ray data from the first set of rats used, which forced us to include a second set of animals), the final *n* for some parameters and some experimental groups was different from that initially set (please see figure legends for ranges). The *n* was set at 4–8 animals per group for the histopathological studies.

Data are presented as the mean values ± SEM. Differences were analyzed using Student's *t*-test with Welch's correction where appropriate, Kruskal–Wallis (followed by Dunn's *post hoc* test) for nonparametric distributions or one-way ANOVA (followed by Bonferroni's *post hoc* test) for parametric distributions, as well as two-way ANOVA followed by Bonferroni's multiple comparison *post hoc* test. Chi-square test was used for evaluating differences in the stomach buoyancy test. Values of *p* < 0.05 were considered significantly different.

3 | RESULTS

3.1 | General health parameters

General health parameters were assessed 8 and 24 h after endotoxin or its vehicle (Figure 1). At 8 h after saline or LPS, all animals had a similar weight loss with respect to T0 (expressed as percentage), without any statistically significant difference among these experimental groups (Figure 1A). At 8 h, the values of the score used to evaluate the clinical status of the rats increased with increasing doses of the endotoxin (Figure 1B), although without reaching statistically significant differences with the control group. At 24 h, all animals treated with LPS showed further weight loss that was statistically significant compared with saline (Figure 1A), and higher clinical score values (Figure 1B), although only animals treated with the highest LPS dose showed statistically significant differences with control and the other groups (Figure 1B).

Mortality of one rat occurred sometime between 8 and 24 h after administration of the highest dose of LPS.

3.2 | Radiographic study

In control rats, the stomach progressively emptied, being almost or completely devoid of barium at 8 and 24 h, respectively (Figure 2A).

GENERAL HEALTH PARAMETERS

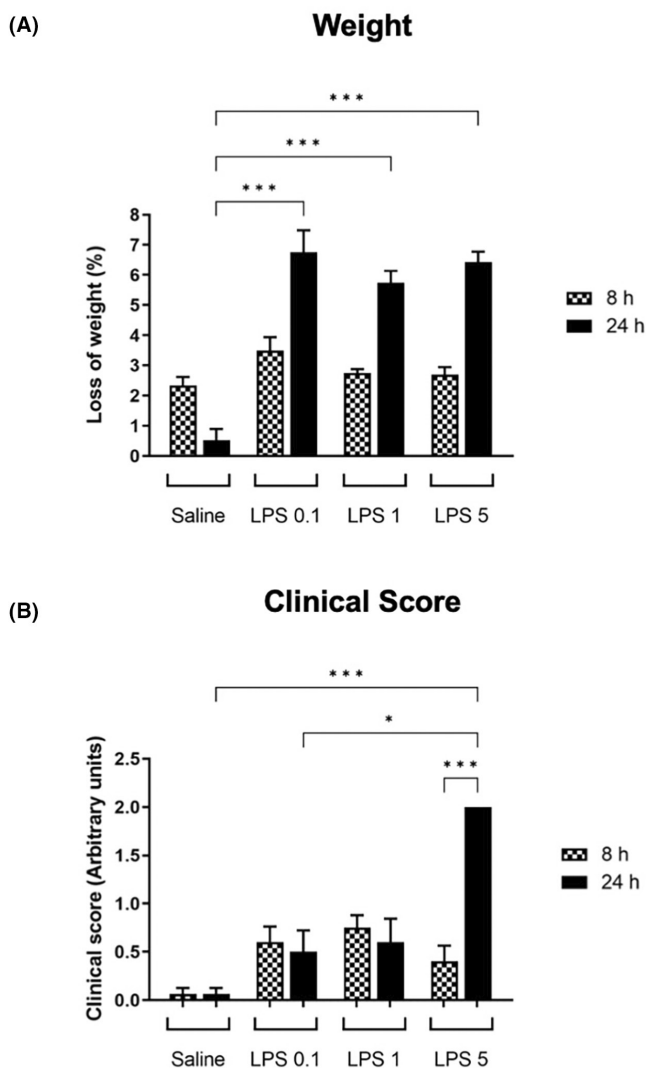


FIGURE 1 Effect of LPS on general health parameters. Rats were weighed (A) and their symptomatology scored (B) before, 8h and 24h after saline (vehicle) or LPS (0.1, 1, or 5 mg kg⁻¹) intraperitoneal (i.p.) administration. Histograms represent mean values \pm SEM ($n=5-12$ per group). * $p < 0.05$, *** $p < 0.001$ (Kruskal-Wallis followed by Dunn's *post hoc* test).

The small intestine contents reached its maximum at 1h. Then, barium contents gradually moved aborally, still being visible (but scarce) at 6–8h (Figure 2B). Once again, at 24h no sign of barium was seen in the small intestine. Cecum started to show radiographic signal 2h after gavage, reaching a maximum from 4 to 8h (Figure 2C) and showing practically no barium at 24h. Colorectum (Figure 2D) started to have barium contents in most animals at 4h, peaked at 8h, and was almost empty at 24h. Figure 2E shows representative images of these findings.

The stomach of LPS-treated rats emptied significantly more slowly than that of control animals, independently from the dose, for the first 8h of the study (Figure 2A). The small intestine was the less affected organ in our experiments. As LPS delayed gastric emptying, small

intestine of animals treated with the low dose showed less contents at 1h, but at 2 and 4h there were no differences compared with control animals (Figure 2B). At 6h, the small intestine of the animals treated with the medium and higher LPS doses was less filled. Finally, at 24h, all animals showed similar absence of barium in this organ.

Compared to control, in animals treated with LPS the cecum started to fill at later points (Figure 2C). In addition, lower scores were reached at every time point, except for 0 and 1h, in which no barium was seen in any animal, and at 24h, in which cecum still showed significant barium contents in all LPS-treated animals. Interestingly, at this time point, the cecum showed higher contents with increasing LPS doses.

Appearance of barium within the colorectum was altered by LPS (Figure 2D) in a similar manner to that observed for the cecum, but dose-dependency of changes was more evident in this organ. From 4 to 24h, LPS retarded colorectum appearance of barium in an inverse dose-dependent manner, with the graph corresponding to LPS 0.1 animals showing the greatest shift to the right compared with control. Despite the delay in reaching the cecum, the graph for LPS at the highest dose overlapped with that for control from 2 to 6h (Figure 2D). Furthermore, in some rats, barium reached the colorectum already 2h after administration of LPS at 1 or 5 mg kg⁻¹ and the stained content did not have a pelleted, but a liquid appearance (see Figure 2E: X-ray taken at 2h shows an illustrative example), which was never seen in control rats or rats treated with LPS at 0.1 mg kg⁻¹. Twenty-four hours after the challenge, the colorectum of LPS-treated animals displayed higher barium contents in comparison to controls, showing a dose-dependent tendency, similar to that in the cecum.

Figure 3 shows data of the morphometric and densitometric study of stomach, cecum, and fecal pellets. Stomach and cecum changes in area and density along time (Figure 3A–D) were in general agreement with the previously described results, except for LPS 5 stomach, which from 1 to 4h showed a significantly bigger area than other doses (Figure 3A). The cecum maximum area (Figure 3C) was significantly lower for LPS-treated animals, irrespective of the dose used, and maximum density of contents in this organ between 4 and 8h (when it was maximum for saline-treated animals) was also reduced compared with controls, but the difference did not reach statistical significance (Figure 3D). However, at 24h, density of cecum in the group treated with LPS 5 was higher than the maximum density reached in control animals and this value decreased in a dose-dependent manner (Figure 3D).

As expected, the number of fecal pellets varied along time in consonance with colorectum contents (Figure 3E). As shown in Figure 3E, for saline-treated animals, this parameter increased from 0 to 5.12 ± 0.4 pellets at 8h and then decreased to 1.65 ± 0.67 pellets at 24h. These pellets had a mean area of 61.52 ± 3.25 mm² (Figure 3F). By contrast, the pellets were fewer in number (at 4–8h) and smaller in LPS than in control animals (Figure 3E,F). However, at 24h there were significantly more feces than in control animals (up to 9.0 ± 1.66 in LPS 0.1, 6 ± 0.95 in LPS 1 and 6.43 ± 1.39 in LPS 5, $p < 0.001$) (Figure 3E). Fecal pellets density did not show any statistically significant differences among the experimental groups (Figure 3G).

RADIOGRAPHIC ANALYSIS

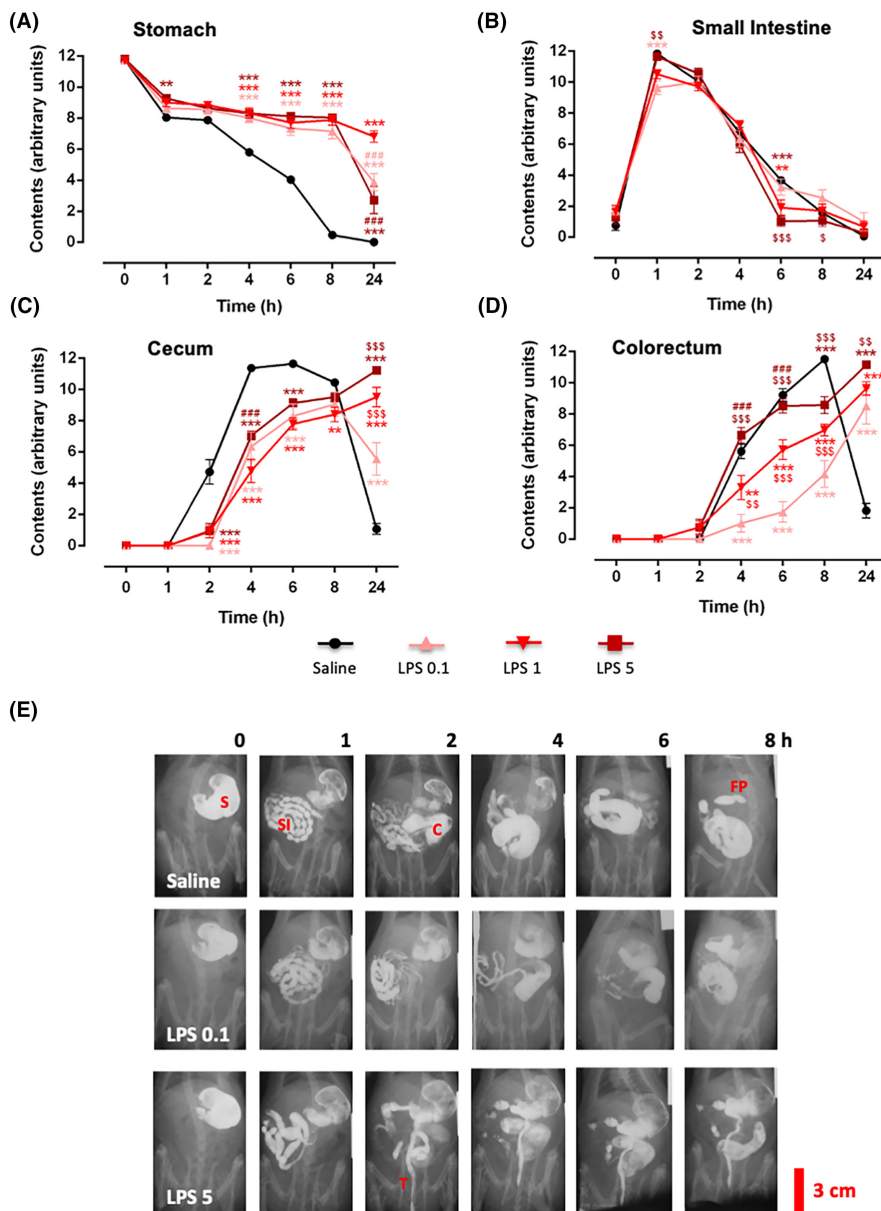


FIGURE 2 Radiographic analysis of the effect of LPS on gastrointestinal motor function in the rat. Rats received an intraperitoneal (i.p.) administration of saline or LPS (0.1, 1, or 5 mg kg⁻¹). After treatment, barium sulfate was administered (2.5 mL and 0.9 g/mL). X-rays were taken immediately and 1, 2, 4, 6, 8, and 24 h after barium. Motility curves show barium transit for the stomach (A), small intestine (B), cecum (C), and colorectum (D), using a semiquantitative score (see Materials and Methods section for details). Data are shown as mean values \pm SEM ($n = 24$ –26 per group). ** $p < 0.01$, *** $p < 0.001$ versus vehicle; \$ $p < 0.05$, \$\$ $p < 0.01$, \$\$\$ $p < 0.001$ versus LPS 0.1; ### $p < 0.001$ versus LPS 1 (2-way ANOVA followed by Bonferroni *post hoc* test). (E) Representative X-ray images of saline, LPS 0.1 and 5 mg kg⁻¹ rats at different time points. Bar scale represents 3 cm. C, cecum; FP, fecal pellets (within the colorectum); S, stomach; SI, small intestine; T, thread appearance of colorectal contents (only seen in LPS 5 images).

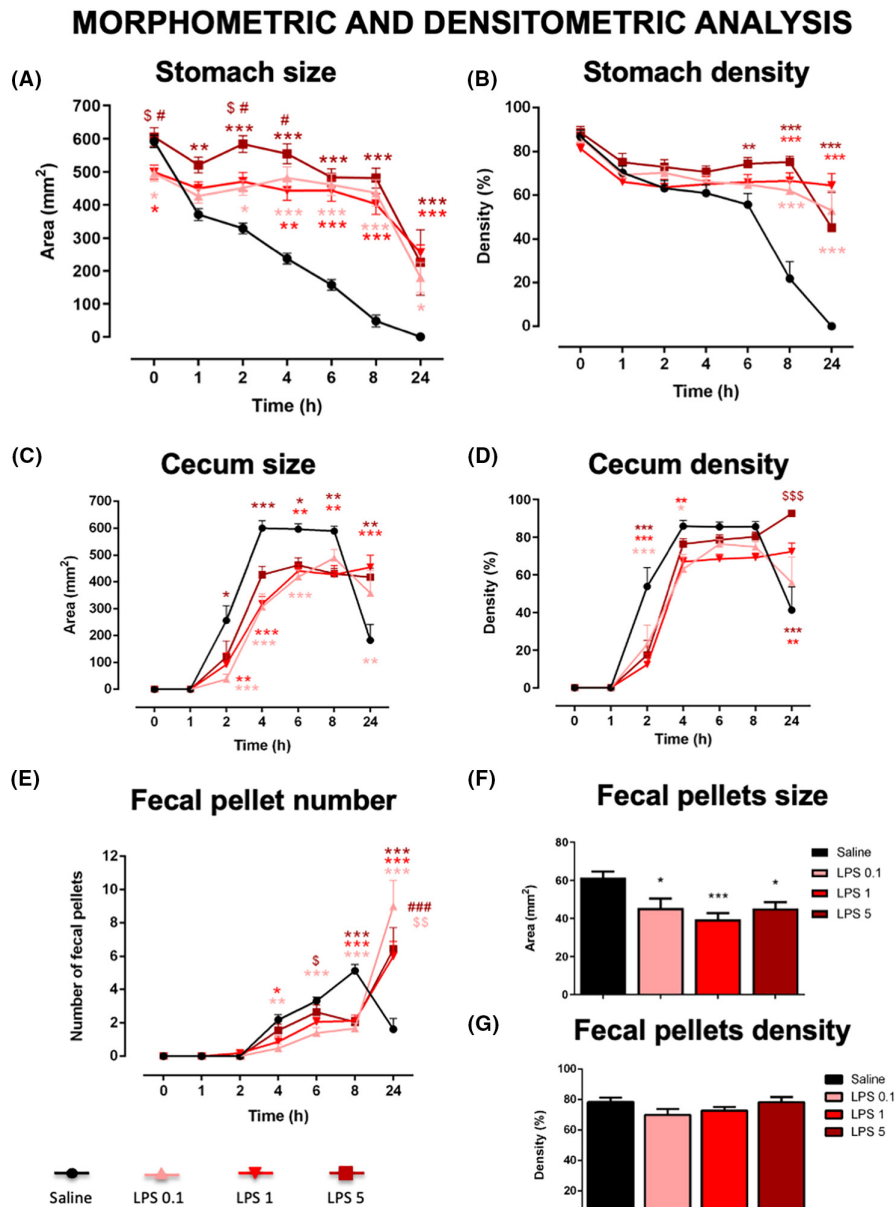
The proportion of animals showing abnormal contents at colorectal level, suggestive of diarrhea,²¹ was also assessed from the X-rays. Only rats treated with the highest dose of LPS showed abnormal colorectal contents (i.e., contents that did not have a normal fecal pellet appearance). Mildly abnormal colorectal content started to be seen at 2 h. Gradually, both the percentage of animals with abnormal content and the severity of this condition increased, reaching a peak of 44% of animals with mild or severe abnormalities at 8 h (Figure 4A).

3.3 | Macroscopic study

Macroscopic analysis of the organs was performed after euthanasia, which took place after the last X-rays were taken at 24 h (Table S1). Comparisons of organ weight and size (area/length) were made after

normalization to body weight, so that the results could be evaluated independently from the effect of LPS on this parameter. LPS tended to decrease liver weight and increase kidney and spleen weight. Statistically significant differences were reached in animals treated with LPS 1 and 5 for spleen or with LPS 5 for kidney. LPS also increased the weight and area of the stomach, the difference reaching statistical significance for LPS 5 (whole stomach area and weight; body and forestomach area). The buoyancy test showed that stomachs from control rats placed in saline sank with no exception, but 44%–66% of the stomachs from LPS rats floated ($p < 0.001$). No macroscopic bleeding was observed in this organ. The endotoxin significantly reduced the area of the cecum at all doses. Nevertheless, no significant differences of cecum weight were observed. The colonic weight (with contents) was significantly reduced in LPS-treated animals. However, LPS did not significantly alter neither the length of the small intestine nor that of the colorectum (Table S1).

FIGURE 3 Morphometric and densitometric analysis of stomach, cecum, and fecal pellets from X-ray images of control and LPS-treated rats. Rats received an intraperitoneal (i.p.) administration of saline or LPS (0.1, 1, or 5 mg kg⁻¹). The area (A) and density (B) of stomach and cecum (C, D) were analyzed in digitized X-rays, as described in Material and Methods section. Fecal pellets were counted (E), and their area and density were also measured (F, G; in these graphs values corresponding to time points 4–24 h after barium were averaged). Data are shown as mean values ± SEM ($n=16-18$ per group). * $p < 0.05$, ** $p < 0.01$, *** $p < 0.001$ versus vehicle; \$ $p < 0.05$, \$\$ $p < 0.01$, \$\$\$ $p < 0.001$ versus LPS 0.1; # $p < 0.05$, ### $p < 0.001$ versus LPS 1 (1 or 2-way ANOVA followed by Bonferroni *post hoc* test or Kruskal–Wallis followed by Dunn's *post hoc* test).



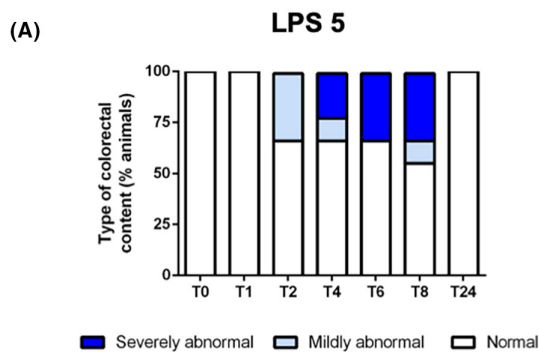
3.4 | Histopathological results

Acute lung injury was shown to be induced in animals exposed to LPS 5 mg kg⁻¹. In these rats, lungs showed alveolar congestion, hemorrhage, and a significant increase in the thickness of their alveolar wall (Figure 4B–D). On the contrary, no significant pathological damage was observed in kidney, esophagus, duodenum, or spleen and only a light infiltration of macrophages was seen in the liver when LPS 5 was used (Figure 4E). The glomerular area of the kidney (μm^2) tended to increase with LPS 5, but the differences among the experimental groups did not reach statistical significance (saline: 9378 ± 608 ; LPS 0.1: 8369 ± 947 ; LPS 1 9477 ± 511 ; LPS 5: $10,342 \pm 119$; $p > 0.05$). By contrast, the stomach, ileum, and distal colon showed some damage (Figures 5 and 6). More precisely, the forestomach showed some hemorrhagic foci in the submucosa of samples of animals treated with LPS 5 (Figure 5A,B). Regarding stomach body, apical damage

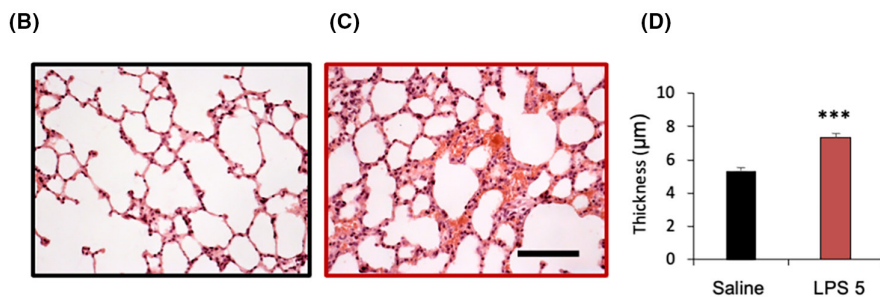
and some basal swelling were observed in glands of animals treated with LPS 5. Additionally, mucosa thickness was smaller in this group (Figure 5C,D). Ileum did not suffer a statistically significant damage in its general architecture (Figures 5E,F and 6A), but the muscle layer thickness was significantly reduced in animals treated with LPS 5 (Figure 6C–E). Finally, the distal colon of animals treated with LPS did not show a significant structural damage (Figure 6B), although some hemorrhagic areas and large Peyer's patches were seen, whereas muscle layer thickness was not significantly altered in LPS 5-treated compared with control animals (Figures 5G,H and 6F–H). The distal colon wall thickness (μm) was not significantly altered by LPS treatment either (saline: 667.1 ± 17 ; LPS 0.1: 711.3 ± 41 ; LPS 1: 683.2 ± 55 ; LPS 5: 682.9 ± 33 ; $p > 0.05$).

Inflammation in colon was further investigated by means of immunohistochemistry. Activated M2 macrophages, immunoreactive to CD-163, were increased in the colonic submucosa in a

Intestinal content appearance



Lung damage



Liver damage

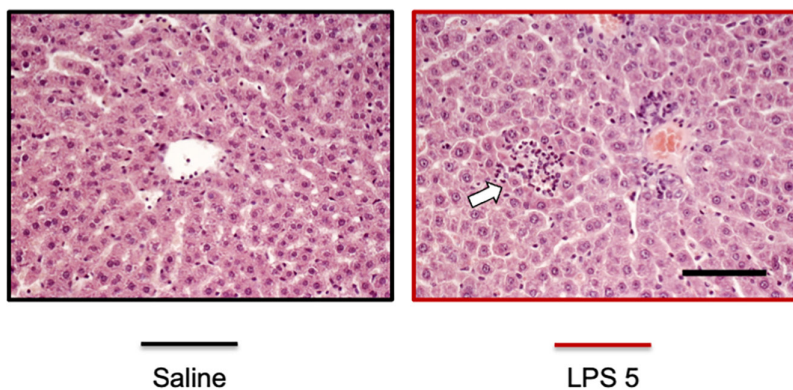


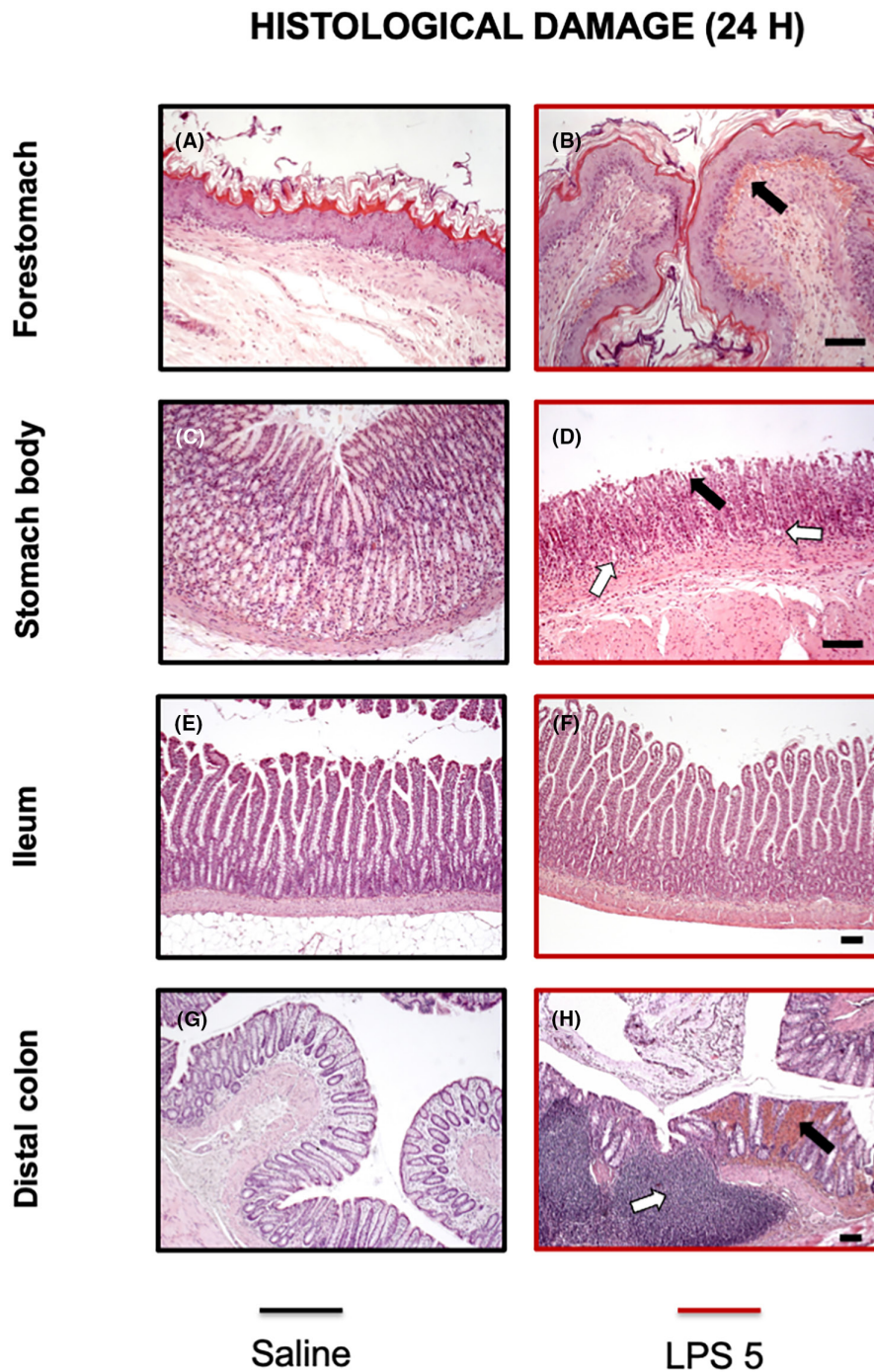
FIGURE 4 Appearance of contents within the colorectum (A), and lung (C–E) and liver (F) damage. (A) Classification of colorectal contents as seen in X-Rays in rats treated with LPS at 5 mg kg^{-1} intraperitoneally (i.p.) (see Material and Methods section for details); $n = 9$ per group. (B) Lung of a control animal treated with saline. (C) Lung of an animal treated with LPS at 5 mg^{-1} (i.p.). (D) Mean thickness \pm SEM of the alveolar wall in saline and LPS 5 animals ($n = 6$ per group), $***p < 0.001$ versus saline (Student's *t*-test). (E) Nodules of immune cells (arrow) in the liver of animals treated with LPS at 5 mg kg^{-1} (i.p.).

dose-dependent manner, and the difference with control was statistically significant for LPS 5 in the distal part (Figure 7A–F). Similarly, the number of MPO-positive neutrophils was significantly increased in the distal colon of the LPS 1 and LPS 5 groups compared with saline-treated animals (Figure 7G–I). Cyclooxygenase-2 labeling changed from a typical basal expression pattern in the epithelial glands of control animals to a generalized expression pattern in the animals treated, especially with the highest dose of the endotoxin, although the differences among control and LPS-treated groups were not statistically significant (Figure 8A–C). Regarding claudin-1 expression, we could not appreciate any remarkable alteration in protein distribution throughout the mucosa, but the intensity of labeling reached significantly higher values in LPS 5-treated animals than in controls and animals treated with LPS 0.1 (Figure 8D,E).

4 | DISCUSSION

The present study shows, using radiographic, noninvasive methods for the first time, the impact of different i.p. doses of the gram-negative bacterial endotoxin LPS on rat gastrointestinal motor function along 24 h. The sepsis-inducer agent produced similar gastric stasis at all doses tested and a biphasic intestinal effect with a brief initial phase of accelerated intestinal transit and a more prolonged and clearly dose-dependent phase of paralytic ileus. Finally, the pathology study performed at 24 h, when significant clinical symptoms (and lung damage) were observed, showed that some of these functional effects, particularly those elicited by low LPS doses, could be produced in the absence of inflammatory damage to the gut wall.

FIGURE 5 Effect of LPS administration on the general structure of the rat stomach, ileum, and distal colon wall. Rats were injected intraperitoneally (i.p.) with saline or LPS at 0.1, 1, or 5 mg kg⁻¹. Histological samples embedded in paraffin sections were obtained 24 h after administration and stained with HE. Left (A, C, E, G): tissue samples from saline-treated animals. Right (B, D, F, H): tissue samples from LPS 5-treated animals. (A,B) general view of the forestomach. Arrow shows hemorrhagic area between the submucosa and *muscularis mucosae* layers. (C,D) stomach body. Epithelial glands are smaller and appear damaged in the LPS 5 animals (black arrow), basal swelling is observed in some of them (white arrow). (E,F) low magnification images of ileum. (G,H) low magnification images of distal colon. In some LPS animals, hemorrhagic *lamina propria* (black arrow) and large Peyer's patches (white arrow) were found. Bar: 100 μm.

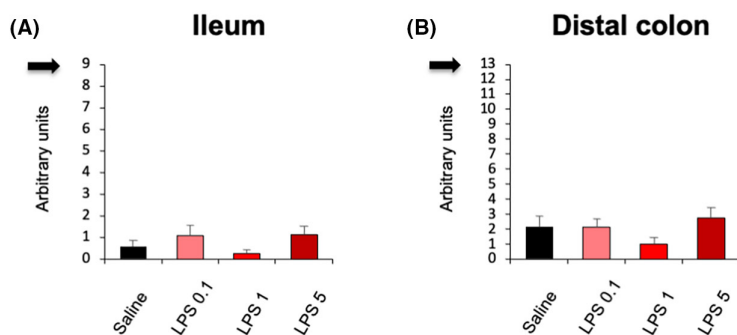


In the gastrointestinal field, doses as low as 0.04 mg kg⁻¹ have been used to evaluate the early effects of LPS on gastric and intestinal motor function.^{30,31} Higher doses (up to 20 mg kg⁻¹) have been used by other authors, but the duration of these studies was always short (less than 24 h)³² due to the fact that mortality increases in a dose-dependent manner.³³ Indeed, in a previous pilot study, mortality at 24 h was absent for animals treated with 0.1, 0.5, 1, and 2.5 mg kg⁻¹, whereas it was 25% (2/8 rats) after 5 mg kg⁻¹ and 75% (3/4 rats) after 10 mg kg⁻¹ (data not shown). Here, mortality was much lower than in our pilot study (3.85%, 1/26 rats treated with LPS 5 mg kg⁻¹), possibly due to the fact that a different batch of LPS was used in the present study.

Rats treated with LPS lost weight and showed signs of dehydration, probably due to less consumption of food and water after treatment, without ruling out as possible causes the concomitant concurrence of diarrhea or the presence of polyuria.³⁴ Anorexia, one of the most described symptoms linked to LPS, may be due to the action of MyD88-dependent proinflammatory cytokines in the brain,³⁵⁻³⁷ but also gastroparesia (see below) may contribute to it and the consequent weight loss.

The response to LPS is known to produce structural damage in several systems, also mimicking the effects of the cytokine storm.³⁸ Thus, LPS at 5 mg kg⁻¹ caused acute lung injury, associated with alveolar congestion, hemorrhage, and a significant increase of

HISTOLOGICAL DAMAGE OF THE INTESTINE



MUSCLE LAYER THICKNESS (24 h)

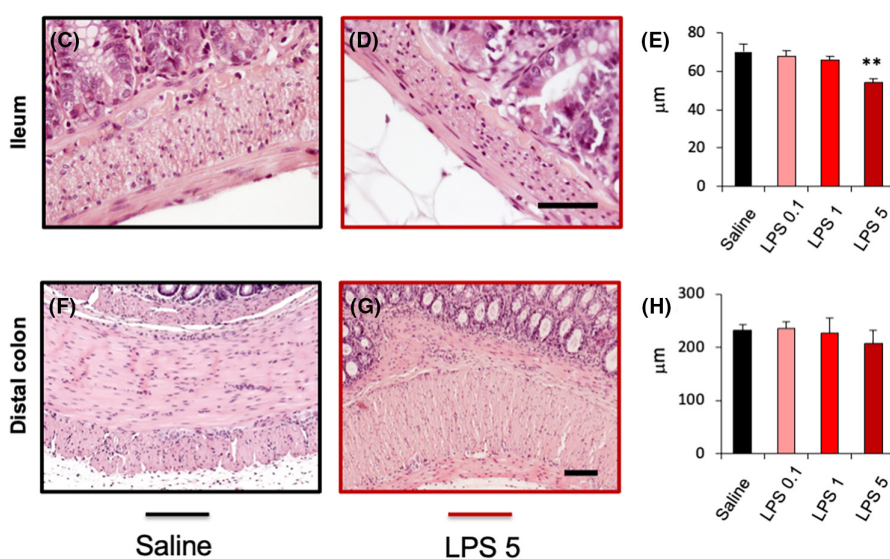


FIGURE 6 Effect of LPS administration on general damage and muscle layer thickness of the rat small intestine and distal colon wall. Rats were injected intraperitoneally (i.p.) with saline or LPS at 0.1, 1, or 5 mg kg⁻¹. Histological samples were obtained 24 h after administration, embedded in paraffin, sectioned and stained with HE. Top panel: general damage of ileum (A) and distal colon (B). Arrows on the OY axis indicate the maximum achievable damage. Bottom panel: Muscle layer thickness at 24 h. Top row (C–E), small intestine. Bottom row (F–H), distal colon. Left (C, F): tissue samples from saline-treated animals. Center (D, G): tissue samples from LPS 5-treated animals. Right (E, H): quantitative analyses. Bars show mean values \pm SEM for control (black), LPS 0.1 (pink), 1 (red), and 5 (dark red) mg kg⁻¹-treated animals. ** $p < 0.01$ versus all other experimental groups (one-way ANOVA followed by Bonferroni *post hoc* test or by Student's *t*-test). $n = 4–8$ per group. Bar: 50 μm for the small intestine samples and 100 μm for the colonic samples.

the alveolar wall thickness 24 h after its intraperitoneal injection. Although intratracheal injection of LPS is often used to cause acute lung injury in rodents, the systemic administration of the endotoxin is also used to mimic sepsis associated with lung damage and cytokine storm; the effects are clearly dependent on the dose and route used, as well as the time point evaluated.^{39–41}

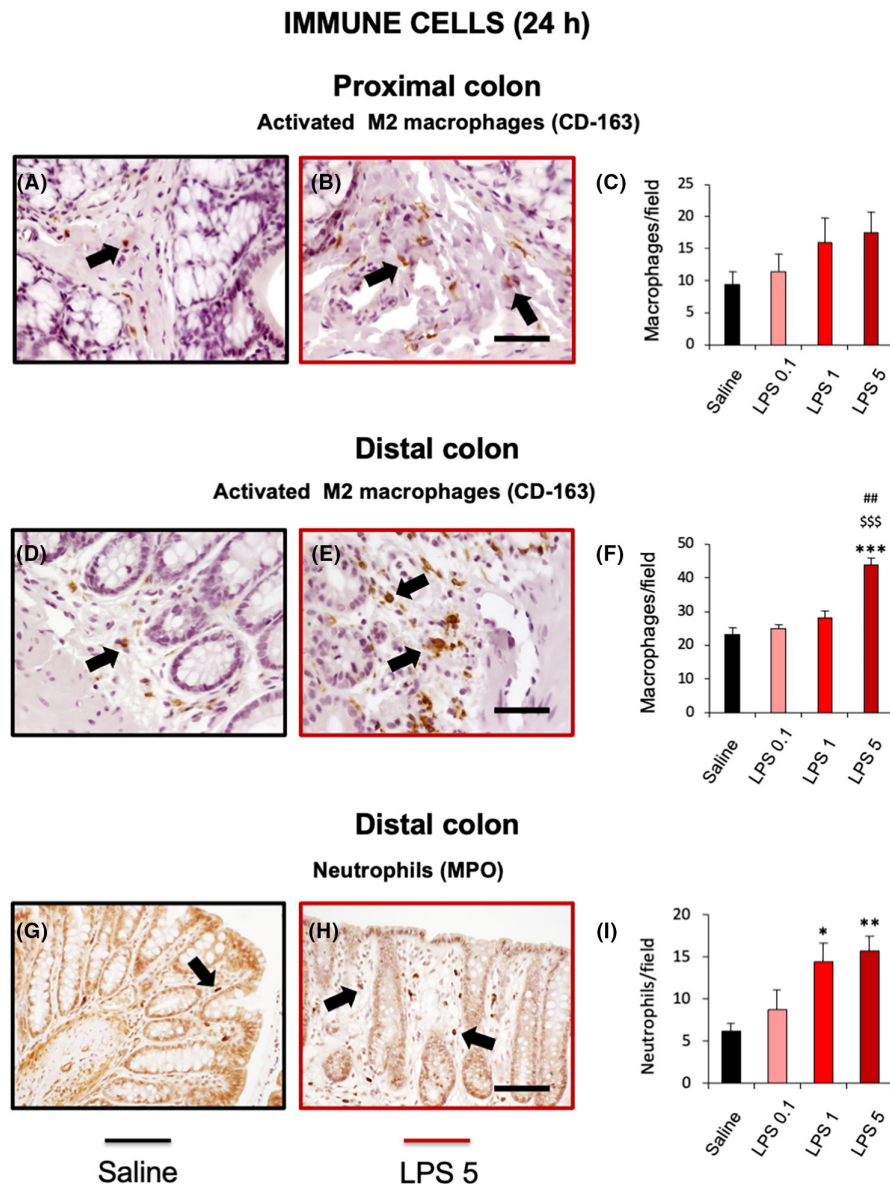
The liver is one of the organs that may be more affected in critically ill patients suffering from paralytic ileus, which may lead to abdominal hypertension and abdominal compartment syndrome.⁷ However, we only found a slight infiltration of macrophages, suggesting that sepsis was at a relatively early stage in our model. Interestingly, LPS has been shown to induce the release of proinflammatory mediators by macrophages in the liver without obvious morphological effects,^{42,43} which is in accordance with our results.

Regarding the kidney, treatment with LPS is an established model to study acute renal failure although usually at higher doses than those we have assayed. Thus, intravenous doses of 20 mg kg⁻¹ in rats have been shown to alter renal blood flow, glomerular filtration rate, and renal function.⁴⁴ Similarly, 15 mg kg⁻¹ i.p. evoked tubular cells

damage, loss of brush border, and apoptosis of nephrons in mice.⁴⁵ In both studies, evaluations were performed 24 h after LPS administration. Doses similar to ours (4 mg kg⁻¹) increased oxidative and apoptosis markers 24 h after LPS administration.⁴⁶ However, histological damage (renal fibrosis) was only described 60 days later. Despite the lack of statistically significant histological damage 24 h after LPS in our study, it cannot be discarded that kidney function was affected, which needs to be specifically studied. Interestingly, in critically ill patients with paralytic ileus, renal function is a strong predictor of intestinal dysmotility, and serum creatinine and intestinal motility were found to be correlated.^{7,47}

Our results show that *E. coli* LPS exerted early and prominent gastric stasis independently of the dose. This organ had increased size (estimated by area) and weight and accumulated gas, likely due to gastric dysmotility. It also showed gastric microbleeding (at 5 mg kg⁻¹), confirming other results obtained with higher doses than ours.⁴⁸ Early gastric stasis has also been described in rats at lower doses, such as 40 $\mu\text{g kg}^{-1}$ ¹³⁰ and in other species, such as sheep,¹⁷ horses,⁴⁹ or dogs,¹⁵ suggesting that gastric hypomotility may be a

FIGURE 7 Effect of LPS administration on the proliferation of immune cells in the rat colon. Rats were injected intraperitoneally (i.p.) with saline or LPS at 0.1, 1, or 5 mg kg⁻¹. Histological samples were obtained 24 h after administration, embedded in paraffin, sectioned and immuno-stained with antibodies against CD163 (A–F) or MPO (G–I). Top row (A–C): proximal colon. Middle (D–F) and bottom (G–I) rows: distal colon. Left (A, D, G): tissue samples from saline-treated animals. Center (B, E, H): colon samples from LPS 5-treated animals. Right (C, F, I): quantitative analyses. Bars show mean values \pm SEM for control (black), LPS 0.1 (pink), 1 (red) and 5 (dark red) mg kg⁻¹-treated animals. * p < 0.05, ** p < 0.01, *** p < 0.001 versus saline; ### p < 0.001 versus LPS 0.1; ## p < 0.01 versus LPS 1 (one-way ANOVA followed by Bonferroni *post hoc* test or Student's *t*-test). n = 4–8 per group. Bar: 50 and 100 μ m for the CD163- and MPO-stained samples, respectively.



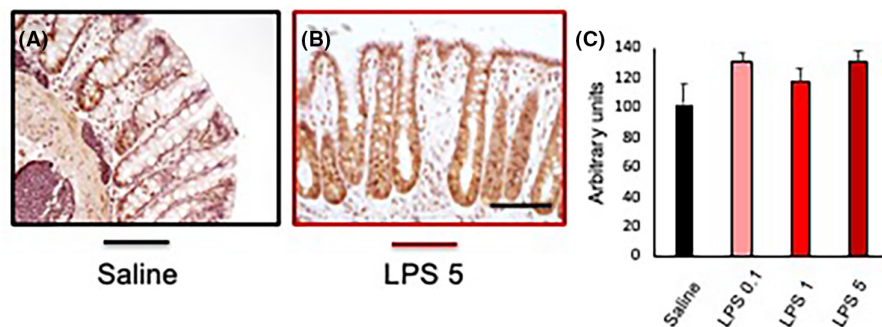
well-conserved basic defense mechanism against (ingested) toxins. In rats, IL-1 β —but not IL-1 or TNF- α —was responsible for antral gastric stasis.⁵⁰ It has been shown that the early gastric response to low doses of LPS may be due to a vagovagal reflex, and the activation of an inhibitory pathway from the dorsal motor complex.^{30,31} Nevertheless, an early upregulation of iNOS may be involved in gastric stasis after endotoxemic doses of LPS similar to ours.⁵¹ The same mechanism has been proposed for the LPS-induced (15 mg kg⁻¹) relaxation of intestinal muscle.⁵²

In our model, 1 h after LPS at 0.1 and 1 mg kg⁻¹ there was a decrease in small intestine contents. This could simply be a consequence of gastric stasis, but it has been demonstrated that doses of 0.1 or 0.4 mg kg⁻¹ reduce the amplitude and frequency of spontaneous spiking activity of rat proximal jejunum, and reduce upper gastrointestinal transit in mice, at an early time point (30–50 min after the administration).¹³ Even if gastric stasis of LPS-treated rats was ongoing, small intestine showed normal contents from 2 to 4 h after LPS. Moreover, the small intestine was already almost empty

of contents earlier in LPS (6 h) than in saline-treated animals (24 h). This suggests that LPS induced some degree of hypermotility of this organ. Although the small intestine was emptied more quickly in LPS-treated animals, filling of cecum was apparently delayed compared with control animals, but, curiously, it was slightly faster for the highest LPS dose. The effect of LPS in the cecum may have been masked by barium dilution. Indeed, the lower semiquantitative score of the cecum at T2 in LPS-treated animals (Figure 2C) seems mainly due to a much lower density of barium in this organ (Figure 3D), compared with the control group. This can be partly explained because there was less barium available to reach and fill the cecum, since less barium reached the small intestine within the first hour of the study, associated with early gastric stasis. However, barium dilution might be also due to a higher accumulation within the cecum of nonstained material (fecal matter and water) in the first few hours after treatment with LPS, due to hypermotility of the small intestine. Moreover, the colorectum was filled in a dose-dependent manner, with the highest dose allowing an even slightly faster filling of this

Distal colon

COX-2 IMMUNOREACTIVITY



CLAUDIN-1 IMMUNOREACTIVITY

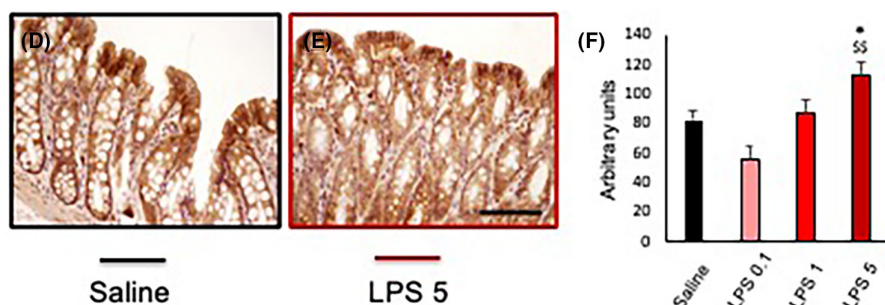


FIGURE 8 Effect of LPS administration on cyclooxygenase-2 (COX-2) and claudin-1 immunoreactivity in the epithelial glands of rat distal colon. Rats were injected intraperitoneally (i.p.) with saline or LPS at 0.1, 1, or 5 mg kg⁻¹. Histological samples were obtained 24 h after administration, embedded in paraffin, sectioned and immuno-stained with antibodies against COX-2 (A,B) or claudin-1 (D,E). A and D: distal colon samples from saline-treated animals. B and E: distal colon samples from LPS 5-treated animals. Bar: 100 μm. C and F: quantitative analyses. Bars show mean intensity values of staining ± SEM for control (black), LPS 0.1 (pink), 1 (red), and 5 (dark red) mg kg⁻¹-treated animals. **p* < 0.05 versus saline, ***p* < 0.01 versus LPS 0.1 (one-way ANOVA followed by Bonferroni *post hoc* test or Student's *t*-test). *n* = 4–8 per group.

organ than in control rats (but only until T4). This, together with the abnormal (diarrheic) appearance of colorectal contents at T2–T8 in some rats, suggests that hypermotility occurred early not only in the small intestine but also in the large intestine, at least in the colorectum. This increase in intestinal transit shortly after LPS is in accordance with other studies in rats treated with low or endotoxemic doses of LPS.^{53–56}

As mentioned above, the cecum was less filled 2 h after LPS despite the apparent increase of small intestine motility. The same delaying effect of LPS in colorectum was observed at 4 h and 6 h for LPS at 0.1 and 1 mg kg⁻¹, and at T8, for all doses. In accordance, fecal pellets decreased in number and area (size), but showed similar density. Ileus is a well-known consequence of endotoxin administration and sepsis.⁵⁷ Our motility data suggest that paralytic ileus was taking place in our model (even if counteracted before T6 by the early hypermotility phase). At 24 h, in both cecum and colorectum, contents were dose-dependently increased in every group of endotoxemic rats compared with control rats, partly due to the barium released from the stomach after LPS gastric effect was reduced, and partly due to the large intestine hypomotility and retention of fecal matter from T8 to the end of the study.

Although LPS can affect intestinal morphology shortly after its administration (30–50 min), when TNF-α and IL-6 blood levels are already increased,¹³ no important histological damage was seen in our model in duodenum, where a moderate inflammatory effect

has been previously described in rats after LPS administration at a dose of 2.5 mg kg⁻¹.⁵⁸ However, in our experimental conditions, the distal parts of the GI tract seem to be more affected by LPS. Thus, we found a thinning of muscle layers that was significant in the ileum at the higher LPS dose assayed, and signs of inflammation in terms of the presence of M2 macrophages and neutrophils, with no signs of epithelial structural damage in the distal colon, where we observed, nevertheless, hemorrhagic foci and an increase in the size and number of Peyer's patches. This is in accordance with other studies in which infiltration of leukocytes in intestinal muscle layers and other markers of inflammation such as iNOS, TNF-α, IL-6, or COX-2 were observed in ileus.^{58–60} Intestinal macrophages such as M2 have been postulated as the primary cells to orchestrate the response to LPS, producing NO or prostaglandins and chemoattractants for leukocytes.^{52,57} Thus, in our model, prostaglandins¹⁷ and NO⁶¹ may be responsible for the slow transit observed. The latter could also be involved in the relaxation of smooth muscle leading to thinning of the muscular layers observed in the ileum and colon of LPS 5 mg kg⁻¹ rats. Besides macrophages and neutrophils, or other cells might also be involved in initial or late ileus phases induced by LPS.^{62,63} The contribution to ileus of other mechanisms, like the activation of the endocannabinoid system,¹³ cannot be discarded.

Lastly, LPS capability to increase epithelial permeability is well-known. Specifically, this propermeability effect has been described

with LPS at a dose of 0.1 mg kg⁻¹, although it was not appreciable until 5 days after its administration and was not associated with any histological damage.⁶⁴ Other authors found an increase in mucosal permeability at a much higher dose (10 mg kg⁻¹), appreciating a decrease in the tight junction proteins.⁶⁵ In our case, we have found an increase in claudin-1 expression in animals treated with LPS at 5 mg kg⁻¹. This is in agreement with other authors who have found claudin-1 upregulation associated with diseases related to increased inflammation and bowel permeability.⁶⁶ Similarly, barrier breakdown seems to be confirmed by the increase in neutrophils⁶⁵ and M2 macrophages.⁶⁷

Our study has several limitations. First, we could not assess the concentrations of blood cytokines, although other researchers have shown increases of cytokines such as IL-1 β , TNF- α , associated with systemic LPS-induced acute lung injury³⁹ and paralytic ileus,⁶⁸ which were found here. Second, despite we attempted to measure the changes in temperature using a rectal thermometer at several time points, the results were inconsistent (data not shown). More accurate methods, like telemetry, will be helpful to confirm the dose-dependent effects of LPS in this parameter described by other researchers⁶⁹⁻⁷¹ Nevertheless, we believe the lack of an adequate measurement of body temperature regarding the monitoring of sepsis evolution does not decrease the interest of our results on gastrointestinal motility, which is the focus of our research. Third, stomach area (size) was not homogenous between groups at T0. As rat weights were comparable, this may be due to the fact that animals were not fasted before experiments (fasting was not applied to avoid stress and discomfort to the rats, because it would have lasted for longer than 24 h). Nevertheless, LPS effect is still remarkably evident in comparison to control (saline) rats, and agree with the literature showing gastric stasis at extremely low LPS doses, as discussed above.^{30,31} Finally, diarrhea was not evaluated using semiquantitative clinical scores like those described by Fukudome et al.⁷² Instead, we relied on the radiographic study, which had previously allowed us to image diarrhea induced by 5-fluorouracil.²¹ Radiographic methods have also allowed to image cannabinoid-mediated paralytic ileus induced by vincristine administration.²⁰ Still, the design of the radiographic study may be optimized to evaluate the effect of LPS on the small and large intestine more specifically, by administering the endotoxin at longer time points after barium gavage, when the organ of interest is already reasonably well filled with contrast (see Bagues et al⁷³ as an example of administration of the challenging insult 1 h after barium).

5 | CONCLUDING REMARKS

Our results suggest that intestinal hypermotility is an early event that increases with the LPS dose and severity of sepsis and somehow counteracts gastrointestinal transit inhibition that leads to ileus and seems to be the “basal effect” of LPS (and relatively dose-independent, as described for the stomach and cecum). More research needs to be done to identify the exact mechanisms involved but, in light of the available scientific literature, it could be

speculated that early hypermotility and diarrhea may be favored by altered motor neurotransmission and/or impaired intestinal water absorption/secretion, whereas thereafter, other mechanisms, probably more directly associated with systemic and local inflammation, may favor ileus predominance.

Using radiographic methods, our study offers, for the first time, an integrated view of LPS-induced gastrointestinal response in conscious animals. The two dysmotility phases identified here correspond well with the clinical findings. Thus, our model may be useful for the assessment of new therapies to treat motor function in septic patients, including smart drugs and drug-release devices able to detect the motility changes and act in a dual manner: first, to counteract hypermotility and diarrhea; second, to counteract ileus and promote efficient motility.

AUTHOR CONTRIBUTIONS

RA designed the study. Parameters on general health were obtained by MC and MSV. MC, MSV, and RG performed the X-ray experiments. MC, MSV, LLG, and RA collected samples. MC, MSV, and YLT performed the X-ray and macroscopic analyses. LLG and JAU performed the histological studies. MC, JAU, and RA wrote the manuscript. MIMF contributed essential intellectual input. MIMF and RA obtained financial support. All authors reviewed and approved the final version of the manuscript.

ACKNOWLEDGMENTS

This work was supported by Ministerio de Ciencia e Innovación (SAF2012-40075-C02-01), Ministerio de Ciencia, Innovación y Universidades (SAF2017-83120-C2-1-R and AGL2017-82987-R), Gobierno de Aragón (B04_17R and B29_17R), Fundación Ibercaja-Universidad de Zaragoza (JIUZ-2015-BIO-02), Comunidad de Madrid (S-SAL/0261/2006; S2010/BMD-2308), and URJC-Banco de Santander (NACfightsCOVID-19).

The authors wish to thank L Blanco, R Franco, J Paredes, A Márquez, C Yáñez, and C Merino for technical assistance, as well as Comunidad Autónoma de Madrid for the technician contract of Lorena Blanco (PEJ15/BIO/TL-0580) and the predoctoral contract of Yolanda López-Tofiño (PEJD-2017-PRE/BMD-3924), and URJC for the predoctoral contract of Yolanda López-Tofiño (under PREDOC20-054 caLL).

CONFLICT OF INTEREST STATEMENT

The authors declare that the research was conducted in the absence of any commercial or financial relationships that could be construed as a potential conflict of interest.

DATA AVAILABILITY STATEMENT

The data that support the findings of this study are available from the corresponding authors upon reasonable request.

ORCID

José A. Uranga  <https://orcid.org/0000-0003-4656-8569>

Raquel Abalo  <https://orcid.org/0000-0002-6726-8795>

REFERENCES

- Genga KR, Russell JA. Update of sepsis in the intensive care unit. *J Innate Immun.* 2017;9:441-455.
- Kaukonen K-M, Bailey M, Suzuki S, Pilcher D, Bellomo R. Mortality related to severe sepsis and septic shock among critically ill patients in Australia and New Zealand, 2000-2012. *JAMA.* 2014;311:1308-1316.
- Gaieski DF, Edwards JM, Kallan MJ, Carr BG. Benchmarking the incidence and mortality of severe sepsis in the United States. *Crit Care Med.* 2013;41:1167-1174.
- Knoop ST, Skrede S, Langeland N, Flaatten HK. Epidemiology and impact on all-cause mortality of sepsis in Norwegian hospitals: A national retrospective study. *PLoS One.* 2017;12:e0187990.
- Nguyen NQ, Ng MP, Chapman M, Fraser RJ, Holloway RH. The impact of admission diagnosis on gastric emptying in critically ill patients. *Crit Care.* 2007;11:R16.
- Caddell KA, Martindale R, McClave SA, Miller K. Can the intestinal dysmotility of critical illness be differentiated from postoperative ileus? *Curr Gastroenterol Rep.* 2011;13:358-367.
- Madl C, Druml W. Systemic consequences of ileus. *Best Pract Res Clin Gastroenterol.* 2003;17:445-456.
- Rhodes A, Evans LE, Alhazzani W, et al. Surviving sepsis campaign: international guidelines for Management of Sepsis and Septic Shock: 2016. *Intensive Care Med.* 2017;43:304-377.
- Gotts JE, Matthay MA. Sepsis: pathophysiology and clinical management. *BMJ.* 2016;353:i1585.
- Wirthlin DJ, Cullen JJ, Spates ST, et al. Gastrointestinal transit during endotoxemia: the role of nitric oxide. *J Surg Res.* 1996;60:307-311.
- Glatzle J, Leutenegger CM, Mueller MH, Kreis ME, Raybould HE, Zittel TT. Mesenteric lymph collected during peritonitis or sepsis potently inhibits gastric motility in rats. *J Gastrointest Surg.* 2004;8:645-652.
- Quintana E, Hernández C, Alvarez-Barrientos A, Esplugues JV, Barrachina MD. Synthesis of nitric oxide in postganglionic myenteric neurons during endotoxemia: implications for gastric motor function in rats. *FASEB J.* 2004;18:531-533.
- Li YY, Li YN, Ni JB, et al. Involvement of cannabinoid-1 and cannabinoid-2 receptors in septic ileus. *Neurogastroenterol Motil.* 2010;22:350-e88.
- Eskandari MK, Kalff JC, Billiar TR, Lee KK, Bauer AJ. Lipopolysaccharide activates the muscularis macrophage network and suppresses circular smooth muscle activity. *Am J Physiol Liver Physiol.* 1997;273:G727-G734.
- Cullen JJ, Caropreso DK, Ephgrave KS. Effect of endotoxin on canine gastrointestinal motility and transit. *J Surg Res.* 1995;58:90-95.
- Spates ST, Cullen JJ, Ephgrave KS, Hinkhouse MM. Effect of Endotoxin on canine colonic motility and transit. *J Gastrointest Surg.* 1998;2:391-398.
- Guerrero-Lindner E, Castro M, Muñoz JM, et al. Central tumour necrosis factor- α mediates the early gastrointestinal motor disturbances induced by lipopolysaccharide in sheep. *Neurogastroenterol Motil.* 2003;15:307-316.
- Cabezas PA, Vera G, Castillo M, Fernández-Pujol R, Martín MI, Abalo R. Radiological study of gastrointestinal motor activity after acute cisplatin in the rat. Temporal relationship with pica. *Auton Neurosci.* 2008;141:54-65.
- Mosińska P, Martín-Ruiz M, González A, et al. Changes in the diet composition of fatty acids and fiber affect the lower gastrointestinal motility but have no impact on cardiovascular parameters: In vivo and in vitro studies. *Neurogastroenterol Motil.* 2019;31:e13651. doi:10.1111/nmo.13651
- Vera G, López-Pérez AE, Uranga JA, Girón R, Martín-Fontelles MI, Abalo R. Involvement of cannabinoid signaling in vincristine-induced gastrointestinal dysmotility in the rat. *Front Pharmacol.* 2017;8:37.
- Abalo R, Uranga JA, Pérez-García I, et al. May cannabinoids prevent the development of chemotherapy-induced diarrhea and intestinal mucositis? Experimental study in the rat. *Neurogastroenterol Motil.* 2017;29:e12952. doi:10.1111/nmo.12952
- Laron Z, Crawford JD. Skin turgor as a quantitative index of dehydration in rats. *Pediatrics.* 1957;19:810-815.
- Vera G, Girón R, Martín-Fontelles MI, Abalo R. Radiographic dose-dependency study of loperamide effects on gastrointestinal motor function in the rat. Temporal relationship with nausea-like behavior. *Neurogastroenterol Motil.* 2019;31:1-14.
- Fahmi ANA, Shehatou GSG, Shebl AM, Salem HA. Febuxostat protects rats against lipopolysaccharide-induced lung inflammation in a dose-dependent manner. *Naunyn Schmiedeberg's Arch Pharmacol.* 2016;389:269-278.
- Martín-Ruiz M, Uranga JA, Mosinska P, et al. Alterations of colonic sensitivity and gastric dysmotility after acute cisplatin and granisetron. *Neurogastroenterol Motil.* 2019;31:e13499.
- Malik NM, Liu YL, Cole N, Sanger GJ, Andrews PLR. Differential effects of dexamethasone, ondansetron and a tachykinin NK1 receptor antagonist (GR205171) on cisplatin-induced changes in behaviour, food intake, pica and gastric function in rats. *Eur J Pharmacol.* 2007;555:164-173.
- Saccani F, Anselmi L, Jaramillo I, Bertoni S, Barocelli E, Sternini C. Protective role of μ opioid receptor activation in intestinal inflammation induced by mesenteric ischemia/reperfusion in mice. *J Neurosci Res.* 2012;90:2146-2153.
- Galeazzi F, Blennerhassett PA, Qiu B, O'Byrne PM, Collins SM. Cigarette smoke aggravates experimental colitis in rats. *Gastroenterology.* 1999;117:877-883.
- Kleiner DE, Brunt EM, Van Natta M, et al. Design and validation of a histological scoring system for nonalcoholic fatty liver disease. *Hepatology.* 2005;41:1313-1321.
- Quintana E, García-Zaragoza E, Angeles Martínez-Cuesta M, Calatayud S, Esplugues JV, Barrachina MD. A cerebral nitrenergic pathway modulates endotoxin-induced changes in gastric motility. *Br J Pharmacol.* 2001;134:325-332.
- Calatayud S, Barrachina MD, García-Zaragoza E, Quintana E, Esplugues JV. Endotoxin inhibits gastric emptying in rats via a capsaicin-sensitive afferent pathway. *Naunyn Schmiedeberg's Arch Pharmacol.* 2001;363:276-280.
- Sun S, Zhang H, Xue B, et al. Protective effect of glutathione against lipopolysaccharide-induced inflammation and mortality in rats. *Inflamm Res.* 2006;55:504-510.
- Soromou L, Jiang L, Wei M, et al. Protection of mice against lipopolysaccharide-induced endotoxic shock by pinocembrin is correlated with regulation of cytokine secretion. *J Immunotoxicol.* 2014;11:56-61.
- Olesen E, de Seigneux S, Wang G, et al. Rapid and segmental specific dysregulation of AQP2, S256-pAQP2 and renal sodium transporters in rats with LPS-induced endotoxaemia. *Nephrol Dial Transplant.* 2009;24:2338-2349.
- Langhans W. Signals generating anorexia during acute illness—symposium on "eating, illness and the gut: is there disorder in the house?". *Proc Nutr Soc.* 2007;66:321-330.
- Ogimoto K, Harris MK, Wisse BE. MyD88 is a key mediator of anorexia, but not weight loss, induced by lipopolysaccharide and interleukin-1 β . *Endocrinology.* 2006;147:4445-4453.
- Von Meyenburg C, Hrupka BH, Arsenijević D, Schwartz GJ, Landmann R, Langhans W. Role for CD14, TLR2, and TLR4 in bacterial product-induced anorexia. *Am J Physiol Regul Integr Comp Physiol.* 2004;287:R298-R305.
- Wang J, Jiang M, Chen X, Montaner LJ. Cytokine storm and leukocyte changes in mild versus severe SARS-CoV-2 infection: review of 3939 COVID-19 patients in China and emerging pathogenesis and therapy concepts. *J Leukoc Biol.* 2020;108:17-41. doi:10.1002/JLB.3COVR0520-272R

39. Li Y, Wu B, Hu C, et al. The role of the vagus nerve on dexmedetomidine promoting survival and lung protection in a sepsis model in rats. *Eur J Pharmacol*. 2022;914:174668.
40. Su X, Wang L, Song Y, Bai C. Inhibition of inflammatory responses by ambroxol, a mucolytic agent, in a murine model of acute lung injury induced by lipopolysaccharide. *Intensive Care Med*. 2004;30:133-140.
41. Domscheit H, Hegeman MA, Carvalho N, Spieth PM. Molecular dynamics of lipopolysaccharide-induced lung injury in rodents. *Front Physiol*. 2020;11:11-36.
42. Tang Y, Bian Z, Zhao L, et al. Interleukin-17 exacerbates hepatic steatosis and inflammation in non-alcoholic fatty liver disease. *Clin Exp Immunol*. 2011;166:281-290.
43. Laskin DL, Gardner CR, Price VF, Jollow DJ. Modulation of macrophage functioning abrogates the acute hepatotoxicity of acetaminophen. *Hepatology*. 1995;21:1045-1050.
44. Gupta A, Rhodes GJ, Berg DT, Gerlitz B, Molitoris BA, Grinnell BW. Activated protein C ameliorates LPS-induced acute kidney injury and downregulates renal INOS and angiotensin 2. *Am J Physiol-renal Physiol*. 2007;293:F245-F254.
45. Chunzhi G, Zunfeng L, Chengwei Q, Xiangmei B, Jingui Y. Hyperin protects against LPS-induced acute kidney injury by inhibiting TLR4 and NLRP3 signaling pathways. *Oncotarget*. 2016;7:82602-82608.
46. Plotnikov EY, Brezgunova AA, Pevzner IB, et al. Mechanisms of LPS-induced acute kidney injury in neonatal and adult rats. *Antioxidants*. 2018;7:105.
47. Barnert J, Dumitrascu D, Neeser G, Doesel S, Wienbeck M. Gastric emptying of a liquid meal in intensive care unit patients. *Gastroenterology*. 1998;114:A865.
48. Ward JL, Adams SD, Delano BA, et al. Ketamine suppresses LPS-induced bile reflux and gastric bleeding in the rat. *J Trauma*. 2010;68:69-75.
49. King JN, Gerring EL. The action of low dose endotoxin on equine bowel motility. *Equine Vet J*. 1991;23:11-17.
50. Tsuchiya Y, Nozu T, Kumei S, Ohhira M, Okumura T. IL-1 receptor antagonist blocks the lipopolysaccharide-induced inhibition of gastric motility in freely moving conscious rats. *Dig Dis Sci*. 2012;57:2555-2561.
51. Takakura K, Hasegawa K, Goto Y, Muramatsu I. Nitric oxide produced by inducible nitric oxide synthase delays gastric emptying in lipopolysaccharide-treated rats. *Anesthesiology*. 1997;87:652-657.
52. Eskandari MK, Kalff JG, Billiar TR, Lee KKW, Bauer AJ. LPS-induced muscularis macrophage nitric oxide suppresses rat jejunal circular muscle activity. *Am J Physiol-Gastrointest Liver Physiol*. 1999;277:G478-G486.
53. Cullen JJ, Mercer D, Hinkhouse M, Ephgrave KS, Conklin JL. Effects of endotoxin on regulation of intestinal smooth muscle nitric oxide synthase and intestinal transit. *Surgery*. 1999;125:339-344.
54. Liu J, Wan R, Xu XF, et al. Effect of Lianshu preparation on lipopolysaccharide-induced diarrhea in rats. *World J Gastroenterol*. 2009;15:2009-2015.
55. Martínez-Cuesta MA, Barrachina MD, Beltrán B, Calatayud S, Esplugues J. Nitric oxide modulates the acute increase of gastrointestinal transit induced by endotoxin in rats: a possible role for tachykinins. *J Pharm Pharmacol*. 1997;49:988-990.
56. Calatayud S, Barrachina MD, Quintana E, Ibiza S, Esplugues JV. Endotoxin stimulates fecal pellet output in rats through a neural mechanism. *Naunyn Schmiedeberg's Arch Pharmacol*. 2003;367:51-55.
57. De Winter BY, De Man JG. Interplay between inflammation, immune system and neuronal pathways: effect on gastrointestinal motility. *World J Gastroenterol*. 2010;16:5523-5535.
58. da Cunha FR, Nardin P, Machado CV, et al. Enteric glial reactivity to systemic LPS administration: changes in GFAP and S100B protein. *Neurosci Res*. 2017;119:15-23.
59. Schwarz NT, Engel B, Eskandari MK, Kalff JC, Grandis JR, Bauer AJ. Lipopolysaccharide preconditioning and cross-tolerance: the induction of protective mechanisms for rat intestinal ileus. *Gastroenterology*. 2002;123:586-598.
60. Schmidt J, Stoffels B, Savanh Chanthaphavong R, Buchholz BM, Nakao A, Bauer AJ. Differential molecular and cellular immune mechanisms of postoperative and LPS-induced ileus in mice and rats. *Cytokine*. 2012;59:49-58.
61. De Winter B. Study of the pathogenesis of paralytic ileus in animal models of experimentally induced postoperative and septic ileus. *Verh K Acad Geneeskdg Belg*. 2003;65:293-324.
62. Buchholz BM, Chanthaphavong RS, Bauer AJM. Nonhemopoietic cell TLR4 signaling is critical in causing early lipopolysaccharide-induced ileus. *J Immunol*. 2009;183:6744-6753.
63. Buchholz BM, Shapiro RA, Vodovotz Y, et al. Myocyte TLR4 enhances enteric and systemic inflammation driving late murine endotoxin ileus. *Am J Physiol Liver Physiol*. 2015;308:G852-G862.
64. Guo S, Al-Sadi R, Said HM, Ma TY. Lipopolysaccharide causes an increase in intestinal tight junction permeability in vitro and in vivo by inducing enterocyte membrane expression and localization of TLR-4 and CD14. *Am J Pathol*. 2013;182:375-387.
65. Zhang L, Wei X, Zhang R, et al. A novel peptide ameliorates LPS-induced intestinal inflammation and mucosal barrier damage via its antioxidant and antiendotoxin effects. *Int J Mol Sci*. 2019;20:3974.
66. Weber CR, Nalle SC, Tretiakova M, Rubin DT, Turner JR. Claudin-1 and claudin-2 expression is elevated in inflammatory bowel disease and may contribute to early neoplastic transformation. *Lab Invest*. 2008;88:1110-1120.
67. Barros MHM, Hauck F, Dreyer JH, Kempkes B, Niedobitek G. Macrophage polarisation: an immunohistochemical approach for identifying M1 and M2 macrophages. *PLoS One*. 2013;8:e80908.
68. Königsrainer I, Türck MH, Eisner F, et al. The gut is not only the target but a source of inflammatory mediators inhibiting gastrointestinal motility during sepsis. *Cell Physiol Biochem*. 2011;28:753-760.
69. Caldwell FT, Graves DB, Wallace BH. Humoral versus neural pathways for fever production in rats after administration of lipopolysaccharide. *J Trauma*. 1999;47:120-129.
70. Dogan MD, Ataoglu H, Akarsu ES. Effects of different serotypes of *Escherichia coli* lipopolysaccharides on body temperature in rats. *Life Sci*. 2000;67:2319-2329.
71. Kupferschmid BJ, Therrien B, Rowsey PJ. Different sickness responses in adult and aged rats following lipopolysaccharide administration. *Biol Res Nurs*. 2018;20:335-342.
72. Fukudome I, Kobayashi M, Dabanaka K, et al. Diamine oxidase as a marker of intestinal mucosal injury and the effect of soluble dietary fiber on gastrointestinal tract toxicity after intravenous 5-fluorouracil treatment in rats. *Med Mol Morphol*. 2014;47:100-107.
73. Bagues A, Lopez-Tofiño Y, Galvez-Robleño C, Abalo R. Effects of two different acute and subchronic stressors on gastrointestinal transit in the rat: a radiographic analysis. *Neurogastroenterol Motil*. 2021;33:e14232.

SUPPORTING INFORMATION

Additional supporting information can be found online in the Supporting Information section at the end of this article.

How to cite this article: Castro M, Valero MS, López-Tofiño Y, et al. Radiographic and histopathological study of gastrointestinal dysmotility in lipopolysaccharide-induced sepsis in the rat. *Neurogastroenterology & Motility*. 2023;35:e14639. doi:[10.1111/nmo.14639](https://doi.org/10.1111/nmo.14639)